

Improved Limits on Lepton Flavor Violating Tau Decays to $\ell\phi$, $\ell\rho$, ℓK^* , and $\ell\bar{K}^*$

B. Aubert,¹ Y. Karyotakis,¹ J. P. Lees,¹ V. Poireau,¹ E. Prencipe,¹ X. Prudent,¹ V. Tisserand,¹ J. Garra Tico,² E. Grauges,² M. Martinelli^{ab,3} A. Palano^{ab,3} M. Pappagallo^{ab,3} G. Eigen,⁴ B. Stugu,⁴ L. Sun,⁴ M. Battaglia,⁵ D. N. Brown,⁵ L. T. Kerth,⁵ Yu. G. Kolomensky,⁵ G. Lynch,⁵ I. L. Osipenkov,⁵ K. Tackmann,⁵ T. Tanabe,⁵ C. M. Hawkes,⁶ N. Soni,⁶ A. T. Watson,⁶ H. Koch,⁷ T. Schroeder,⁷ D. J. Asgeirsson,⁸ B. G. Fulsom,⁸ C. Hearty,⁸ T. S. Mattison,⁸ J. A. McKenna,⁸ M. Barrett,⁹ A. Khan,⁹ A. Randle-Conde,⁹ V. E. Blinov,¹⁰ A. D. Bukin,^{10,*} A. R. Buzykaev,¹⁰ V. P. Druzhinin,¹⁰ V. B. Golubev,¹⁰ A. P. Onuchin,¹⁰ S. I. Serednyakov,¹⁰ Yu. I. Skovpen,¹⁰ E. P. Solodov,¹⁰ K. Yu. Todyshev,¹⁰ M. Bondioli,¹¹ S. Curry,¹¹ I. Eschrich,¹¹ D. Kirkby,¹¹ A. J. Lankford,¹¹ P. Lund,¹¹ M. Mandelkern,¹¹ E. C. Martin,¹¹ D. P. Stoker,¹¹ S. Abachi,¹² C. Buchanan,¹² H. Atmacan,¹³ J. W. Gary,¹³ F. Liu,¹³ O. Long,¹³ G. M. Vitug,¹³ Z. Yasin,¹³ L. Zhang,¹³ V. Sharma,¹⁴ C. Campagnari,¹⁵ T. M. Hong,¹⁵ D. Kovalskyi,¹⁵ M. A. Mazur,¹⁵ J. D. Richman,¹⁵ T. W. Beck,¹⁶ A. M. Eisner,¹⁶ C. A. Heusch,¹⁶ J. Kroseberg,¹⁶ W. S. Lockman,¹⁶ A. J. Martinez,¹⁶ T. Schalk,¹⁶ B. A. Schumm,¹⁶ A. Seiden,¹⁶ L. O. Winstrom,¹⁶ C. H. Cheng,¹⁷ D. A. Doll,¹⁷ B. Echenard,¹⁷ F. Fang,¹⁷ D. G. Hitlin,¹⁷ I. Narsky,¹⁷ T. Piatenko,¹⁷ F. C. Porter,¹⁷ R. Andreassen,¹⁸ G. Mancinelli,¹⁸ B. T. Meadows,¹⁸ K. Mishra,¹⁸ M. D. Sokoloff,¹⁸ P. C. Bloom,¹⁹ W. T. Ford,¹⁹ A. Gaz,¹⁹ J. F. Hirschauer,¹⁹ M. Nagel,¹⁹ U. Nauenberg,¹⁹ J. G. Smith,¹⁹ S. R. Wagner,¹⁹ R. Ayad,^{20,†} A. Soffer,^{20,‡} W. H. Toki,²⁰ R. J. Wilson,²⁰ E. Feltresi,²¹ A. Hauke,²¹ H. Jasper,²¹ T. M. Karbach,²¹ J. Merkel,²¹ A. Petzold,²¹ B. Spaan,²¹ K. Wacker,²¹ M. J. Kobel,²² R. Nogowski,²² K. R. Schubert,²² R. Schwierz,²² A. Volk,²² D. Bernard,²³ G. R. Bonneaud,²³ E. Latour,²³ M. Verderi,²³ P. J. Clark,²⁴ S. Playfer,²⁴ J. E. Watson,²⁴ M. Andreotti^{ab,25} D. Bettoni^{a,25} C. Bozzi^{a,25} R. Calabrese^{ab,25} A. Cecchi^{ab,25} G. Cibinetto^{ab,25} E. Fioravanti^{ab,25} P. Franchini^{ab,25} E. Luppi^{ab,25} M. Munerato^{ab,25} M. Negrini^{ab,25} A. Petrella^{ab,25} L. Piemontese^{a,25} V. Santoro^{ab,25} R. Baldini-Ferroli,²⁶ A. Calcaterra,²⁶ R. de Sangro,²⁶ G. Finocchiaro,²⁶ S. Pacetti,²⁶ P. Patteri,²⁶ I. M. Peruzzi,^{26,§} M. Piccolo,²⁶ M. Rama,²⁶ A. Zallo,²⁶ R. Contri^{ab,27} E. Guido,²⁷ M. Lo Vetere^{ab,27} M. R. Monge^{ab,27} S. Passaggio^{a,27} C. Patrignani^{ab,27} E. Robutti^{a,27} S. Tosi^{ab,27} K. S. Chaisanguanthum,²⁸ M. Morii,²⁸ A. Adametz,²⁹ J. Marks,²⁹ S. Schenk,²⁹ U. Uwer,²⁹ F. U. Bernlochner,³⁰ V. Klose,³⁰ H. M. Lacker,³⁰ D. J. Bard,³¹ P. D. Dauncey,³¹ M. Tibbetts,³¹ P. K. Behera,³² M. J. Charles,³² U. Mallik,³² J. Cochran,³³ H. B. Crawley,³³ L. Dong,³³ V. Eyges,³³ W. T. Meyer,³³ S. Prell,³³ E. I. Rosenberg,³³ A. E. Rubin,³³ Y. Y. Gao,³⁴ A. V. Gritsan,³⁴ Z. J. Guo,³⁴ N. Arnaud,³⁵ J. Béquilleux,³⁵ A. D'Orazio,³⁵ M. Davier,³⁵ D. Derkach,³⁵ J. Firmino da Costa,³⁵ G. Grosdidier,³⁵ F. Le Diberder,³⁵ V. Lepeltier,³⁵ A. M. Lutz,³⁵ B. Malaescu,³⁵ S. Pruvot,³⁵ P. Roudeau,³⁵ M. H. Schune,³⁵ J. Serrano,³⁵ V. Sordini,^{35,¶} A. Stocchi,³⁵ G. Wormser,³⁵ D. J. Lange,³⁶ D. M. Wright,³⁶ I. Bingham,³⁷ J. P. Burke,³⁷ C. A. Chavez,³⁷ J. R. Fry,³⁷ E. Gabathuler,³⁷ R. Gamet,³⁷ D. E. Hutchcroft,³⁷ D. J. Payne,³⁷ C. Touramanis,³⁷ A. J. Bevan,³⁸ C. K. Clarke,³⁸ F. Di Lodovico,³⁸ R. Sacco,³⁸ M. Sigamani,³⁸ G. Cowan,³⁹ S. Paramesvaran,³⁹ A. C. Wren,³⁹ D. N. Brown,⁴⁰ C. L. Davis,⁴⁰ A. G. Denig,⁴¹ M. Fritsch,⁴¹ W. Gradl,⁴¹ A. Hafner,⁴¹ K. E. Alwyn,⁴² D. Bailey,⁴² R. J. Barlow,⁴² G. Jackson,⁴² G. D. Lafferty,⁴² T. J. West,⁴² J. I. Yi,⁴² J. Anderson,⁴³ C. Chen,⁴³ A. Jawahery,⁴³ D. A. Roberts,⁴³ G. Simi,⁴³ J. M. Tuggle,⁴³ C. Dallapiccola,⁴⁴ E. Salvati,⁴⁴ S. Saremi,⁴⁴ R. Cowan,⁴⁵ D. Dujmic,⁴⁵ P. H. Fisher,⁴⁵ S. W. Henderson,⁴⁵ G. Sciolla,⁴⁵ M. Spitznagel,⁴⁵ R. K. Yamamoto,⁴⁵ M. Zhao,⁴⁵ P. M. Patel,⁴⁶ S. H. Robertson,⁴⁶ M. Schram,⁴⁶ A. Lazzaro^{ab,47} V. Lombardo^{a,47} F. Palombo^{ab,47} S. Stracka^{ab,47} J. M. Bauer,⁴⁸ L. Cremaldi,⁴⁸ R. Godang,^{48,**} R. Kroeger,⁴⁸ D. J. Summers,⁴⁸ H. W. Zhao,⁴⁸ M. Simard,⁴⁹ P. Taras,⁴⁹ H. Nicholson,⁵⁰ G. De Nardo^{ab,51} L. Lista^{a,51} D. Monorchio^{ab,51} G. Onorato^{ab,51} C. Sciacca^{ab,51} G. Raven,⁵² H. L. Snoek,⁵² C. P. Jessop,⁵³ K. J. Knoepfel,⁵³ J. M. LoSecco,⁵³ W. F. Wang,⁵³ L. A. Corwin,⁵⁴ K. Honscheid,⁵⁴ H. Kagan,⁵⁴ R. Kass,⁵⁴ J. P. Morris,⁵⁴ A. M. Rahimi,⁵⁴ J. J. Regensburger,⁵⁴ S. J. Sekula,⁵⁴ Q. K. Wong,⁵⁴ N. L. Blount,⁵⁵ J. Brau,⁵⁵ R. Frey,⁵⁵ O. Igonkina,⁵⁵ J. A. Kolb,⁵⁵ M. Lu,⁵⁵ R. Rahmat,⁵⁵ N. B. Sinev,⁵⁵ D. Strom,⁵⁵ J. Strube,⁵⁵ E. Torrence,⁵⁵ G. Castelli^{ab,56} N. Gagliardi^{ab,56} M. Margoni^{ab,56} M. Morandin^{a,56} M. Posocco^{a,56} M. Rotondo^{a,56} F. Simonetto^{ab,56} R. Stroili^{ab,56} C. Voci^{ab,56} P. del Amo Sanchez,⁵⁷ E. Ben-Haim,⁵⁷ H. Briand,⁵⁷ J. Chauveau,⁵⁷ O. Hamon,⁵⁷ Ph. Leruste,⁵⁷ G. Marchiori,⁵⁷ J. Ocariz,⁵⁷ A. Perez,⁵⁷ J. Prendki,⁵⁷ S. Sitt,⁵⁷ L. Gladney,⁵⁸ M. Biasini^{ab,59} E. Manoni^{ab,59} C. Angelini^{ab,60} G. Batignani^{ab,60} S. Bettarini^{ab,60} G. Calderini^{ab,60,††} M. Carpinelli^{ab,60,‡‡} A. Cervelli^{ab,60} F. Forti^{ab,60} M. A. Giorgi^{ab,60} A. Lusiani^{ac,60} M. Morganti^{ab,60} N. Neri^{ab,60} E. Paoloni^{ab,60} G. Rizzo^{ab,60} J. J. Walsh^{a,60}

D. Lopes Pegna,⁶¹ C. Lu,⁶¹ J. Olsen,⁶¹ A. J. S. Smith,⁶¹ A. V. Telnov,⁶¹ F. Anulli^a,⁶² E. Baracchini^{ab},⁶² G. Cavoto^a,⁶² R. Faccini^{ab},⁶² F. Ferrarotto^a,⁶² F. Ferroni^{ab},⁶² M. Gaspero^{ab},⁶² P. D. Jackson^a,⁶² L. Li Gioi^a,⁶² M. A. Mazzoni^a,⁶² S. Morganti^a,⁶² G. Piredda^a,⁶² F. Renga^{ab},⁶² C. Voena^a,⁶² M. Ebert,⁶³ T. Hartmann,⁶³ H. Schröder,⁶³ R. Waldi,⁶³ T. Adye,⁶⁴ B. Franek,⁶⁴ E. O. Olaiya,⁶⁴ F. F. Wilson,⁶⁴ S. Emery,⁶⁵ L. Esteve,⁶⁵ G. Hamel de Monchenault,⁶⁵ W. Kozanecki,⁶⁵ G. Vasseur,⁶⁵ Ch. Yèche,⁶⁵ M. Zito,⁶⁵ M. T. Allen,⁶⁶ D. Aston,⁶⁶ R. Bartoldus,⁶⁶ J. F. Benitez,⁶⁶ R. Cenci,⁶⁶ J. P. Coleman,⁶⁶ M. R. Convery,⁶⁶ J. C. Dingfelder,⁶⁶ J. Dorfan,⁶⁶ G. P. Dubois-Felsmann,⁶⁶ W. Dunwoodie,⁶⁶ R. C. Field,⁶⁶ A. M. Gabareen,⁶⁶ M. T. Graham,⁶⁶ P. Grenier,⁶⁶ C. Hast,⁶⁶ W. R. Innes,⁶⁶ J. Kaminski,⁶⁶ M. H. Kelsey,⁶⁶ H. Kim,⁶⁶ P. Kim,⁶⁶ M. L. Kocian,⁶⁶ D. W. G. S. Leith,⁶⁶ S. Li,⁶⁶ B. Lindquist,⁶⁶ S. Luitz,⁶⁶ V. Luth,⁶⁶ H. L. Lynch,⁶⁶ D. B. MacFarlane,⁶⁶ H. Marsiske,⁶⁶ R. Messner,^{66,*} D. R. Muller,⁶⁶ H. Neal,⁶⁶ S. Nelson,⁶⁶ C. P. O'Grady,⁶⁶ I. Ofte,⁶⁶ M. Perl,⁶⁶ B. N. Ratcliff,⁶⁶ A. Roodman,⁶⁶ A. A. Salnikov,⁶⁶ R. H. Schindler,⁶⁶ J. Schwiening,⁶⁶ A. Snyder,⁶⁶ D. Su,⁶⁶ M. K. Sullivan,⁶⁶ K. Suzuki,⁶⁶ S. K. Swain,⁶⁶ J. M. Thompson,⁶⁶ J. Va'vra,⁶⁶ A. P. Wagner,⁶⁶ M. Weaver,⁶⁶ C. A. West,⁶⁶ W. J. Wisniewski,⁶⁶ M. Wittgen,⁶⁶ D. H. Wright,⁶⁶ H. W. Wulsin,⁶⁶ A. K. Yarritu,⁶⁶ K. Yi,⁶⁶ C. C. Young,⁶⁶ V. Ziegler,⁶⁶ X. R. Chen,⁶⁷ H. Liu,⁶⁷ W. Park,⁶⁷ M. V. Purohit,⁶⁷ R. M. White,⁶⁷ J. R. Wilson,⁶⁷ P. R. Burchat,⁶⁸ A. J. Edwards,⁶⁸ T. S. Miyashita,⁶⁸ S. Ahmed,⁶⁹ M. S. Alam,⁶⁹ J. A. Ernst,⁶⁹ B. Pan,⁶⁹ M. A. Saeed,⁶⁹ S. B. Zain,⁶⁹ S. M. Spanier,⁷⁰ B. J. Wogsland,⁷⁰ R. Eckmann,⁷¹ J. L. Ritchie,⁷¹ A. M. Ruland,⁷¹ C. J. Schilling,⁷¹ R. F. Schwitters,⁷¹ B. C. Wray,⁷¹ B. W. Drummond,⁷² J. M. Izen,⁷² X. C. Lou,⁷² F. Bianchi^{ab},⁷³ D. Gamba^{ab},⁷³ M. Pelliccioni^{ab},⁷³ M. Bomben^{ab},⁷⁴ L. Bosisio^{ab},⁷⁴ C. Cartaro^{ab},⁷⁴ G. Della Ricca^{ab},⁷⁴ L. Lancieri^{ab},⁷⁴ L. Vitale^{ab},⁷⁴ V. Azzolini,⁷⁵ N. Lopez-March,⁷⁵ F. Martinez-Vidal,⁷⁵ D. A. Milanese,⁷⁵ A. Oyanguren,⁷⁵ J. Albert,⁷⁶ Sw. Banerjee,⁷⁶ B. Bhuyan,⁷⁶ H. H. F. Choi,⁷⁶ K. Hamano,⁷⁶ G. J. King,⁷⁶ R. Kowalewski,⁷⁶ M. J. Lewczuk,⁷⁶ I. M. Nugent,⁷⁶ J. M. Roney,⁷⁶ R. J. Sobie,⁷⁶ T. J. Gershon,⁷⁷ P. F. Harrison,⁷⁷ J. Ilic,⁷⁷ T. E. Latham,⁷⁷ G. B. Mohanty,⁷⁷ E. M. T. Puccio,⁷⁷ H. R. Band,⁷⁸ X. Chen,⁷⁸ S. Dasu,⁷⁸ K. T. Flood,⁷⁸ Y. Pan,⁷⁸ R. Prepost,⁷⁸ C. O. Vuosalo,⁷⁸ and S. L. Wu⁷⁸

(The BABAR Collaboration)

¹Laboratoire d'Annecy-le-Vieux de Physique des Particules (LAPP),

Université de Savoie, CNRS/IN2P3, F-74941 Annecy-Le-Vieux, France

²Universitat de Barcelona, Facultat de Física, Departament ECM, E-08028 Barcelona, Spain

³INFN Sezione di Bari^a; Dipartimento di Fisica, Università di Bari^b, I-70126 Bari, Italy

⁴University of Bergen, Institute of Physics, N-5007 Bergen, Norway

⁵Lawrence Berkeley National Laboratory and University of California, Berkeley, California 94720, USA

⁶University of Birmingham, Birmingham, B15 2TT, United Kingdom

⁷Ruhr Universität Bochum, Institut für Experimentalphysik 1, D-44780 Bochum, Germany

⁸University of British Columbia, Vancouver, British Columbia, Canada V6T 1Z1

⁹Brunel University, Uxbridge, Middlesex UB8 3PH, United Kingdom

¹⁰Budker Institute of Nuclear Physics, Novosibirsk 630090, Russia

¹¹University of California at Irvine, Irvine, California 92697, USA

¹²University of California at Los Angeles, Los Angeles, California 90024, USA

¹³University of California at Riverside, Riverside, California 92521, USA

¹⁴University of California at San Diego, La Jolla, California 92093, USA

¹⁵University of California at Santa Barbara, Santa Barbara, California 93106, USA

¹⁶University of California at Santa Cruz, Institute for Particle Physics, Santa Cruz, California 95064, USA

¹⁷California Institute of Technology, Pasadena, California 91125, USA

¹⁸University of Cincinnati, Cincinnati, Ohio 45221, USA

¹⁹University of Colorado, Boulder, Colorado 80309, USA

²⁰Colorado State University, Fort Collins, Colorado 80523, USA

²¹Technische Universität Dortmund, Fakultät Physik, D-44221 Dortmund, Germany

²²Technische Universität Dresden, Institut für Kern- und Teilchenphysik, D-01062 Dresden, Germany

²³Laboratoire Leprince-Ringuet, CNRS/IN2P3, Ecole Polytechnique, F-91128 Palaiseau, France

²⁴University of Edinburgh, Edinburgh EH9 3JZ, United Kingdom

²⁵INFN Sezione di Ferrara^a; Dipartimento di Fisica, Università di Ferrara^b, I-44100 Ferrara, Italy

²⁶INFN Laboratori Nazionali di Frascati, I-00044 Frascati, Italy

²⁷INFN Sezione di Genova^a; Dipartimento di Fisica, Università di Genova^b, I-16146 Genova, Italy

²⁸Harvard University, Cambridge, Massachusetts 02138, USA

²⁹Universität Heidelberg, Physikalisches Institut, Philosophenweg 12, D-69120 Heidelberg, Germany

³⁰Humboldt-Universität zu Berlin, Institut für Physik, Newtonstr. 15, D-12489 Berlin, Germany

³¹Imperial College London, London, SW7 2AZ, United Kingdom

³²University of Iowa, Iowa City, Iowa 52242, USA

³³Iowa State University, Ames, Iowa 50011-3160, USA

³⁴Johns Hopkins University, Baltimore, Maryland 21218, USA

- ³⁵Laboratoire de l'Accélérateur Linéaire, IN2P3/CNRS et Université Paris-Sud 11, Centre Scientifique d'Orsay, B. P. 34, F-91898 Orsay Cedex, France
- ³⁶Lawrence Livermore National Laboratory, Livermore, California 94550, USA
- ³⁷University of Liverpool, Liverpool L69 7ZE, United Kingdom
- ³⁸Queen Mary, University of London, London, E1 4NS, United Kingdom
- ³⁹University of London, Royal Holloway and Bedford New College, Egham, Surrey TW20 0EX, United Kingdom
- ⁴⁰University of Louisville, Louisville, Kentucky 40292, USA
- ⁴¹Johannes Gutenberg-Universität Mainz, Institut für Kernphysik, D-55099 Mainz, Germany
- ⁴²University of Manchester, Manchester M13 9PL, United Kingdom
- ⁴³University of Maryland, College Park, Maryland 20742, USA
- ⁴⁴University of Massachusetts, Amherst, Massachusetts 01003, USA
- ⁴⁵Massachusetts Institute of Technology, Laboratory for Nuclear Science, Cambridge, Massachusetts 02139, USA
- ⁴⁶McGill University, Montréal, Québec, Canada H3A 2T8
- ⁴⁷INFN Sezione di Milano^a; Dipartimento di Fisica, Università di Milano^b, I-20133 Milano, Italy
- ⁴⁸University of Mississippi, University, Mississippi 38677, USA
- ⁴⁹Université de Montréal, Physique des Particules, Montréal, Québec, Canada H3C 3J7
- ⁵⁰Mount Holyoke College, South Hadley, Massachusetts 01075, USA
- ⁵¹INFN Sezione di Napoli^a; Dipartimento di Scienze Fisiche, Università di Napoli Federico II^b, I-80126 Napoli, Italy
- ⁵²NIKHEF, National Institute for Nuclear Physics and High Energy Physics, NL-1009 DB Amsterdam, The Netherlands
- ⁵³University of Notre Dame, Notre Dame, Indiana 46556, USA
- ⁵⁴Ohio State University, Columbus, Ohio 43210, USA
- ⁵⁵University of Oregon, Eugene, Oregon 97403, USA
- ⁵⁶INFN Sezione di Padova^a; Dipartimento di Fisica, Università di Padova^b, I-35131 Padova, Italy
- ⁵⁷Laboratoire de Physique Nucléaire et de Hautes Energies, IN2P3/CNRS, Université Pierre et Marie Curie-Paris6, Université Denis Diderot-Paris7, F-75252 Paris, France
- ⁵⁸University of Pennsylvania, Philadelphia, Pennsylvania 19104, USA
- ⁵⁹INFN Sezione di Perugia^a; Dipartimento di Fisica, Università di Perugia^b, I-06100 Perugia, Italy
- ⁶⁰INFN Sezione di Pisa^a; Dipartimento di Fisica, Università di Pisa^b; Scuola Normale Superiore di Pisa^c, I-56127 Pisa, Italy
- ⁶¹Princeton University, Princeton, New Jersey 08544, USA
- ⁶²INFN Sezione di Roma^a; Dipartimento di Fisica, Università di Roma La Sapienza^b, I-00185 Roma, Italy
- ⁶³Universität Rostock, D-18051 Rostock, Germany
- ⁶⁴Rutherford Appleton Laboratory, Chilton, Didcot, Oxon, OX11 0QX, United Kingdom
- ⁶⁵CEA, Irfu, SPP, Centre de Saclay, F-91191 Gif-sur-Yvette, France
- ⁶⁶SLAC National Accelerator Laboratory, Stanford, California 94309 USA
- ⁶⁷University of South Carolina, Columbia, South Carolina 29208, USA
- ⁶⁸Stanford University, Stanford, California 94305-4060, USA
- ⁶⁹State University of New York, Albany, New York 12222, USA
- ⁷⁰University of Tennessee, Knoxville, Tennessee 37996, USA
- ⁷¹University of Texas at Austin, Austin, Texas 78712, USA
- ⁷²University of Texas at Dallas, Richardson, Texas 75083, USA
- ⁷³INFN Sezione di Torino^a; Dipartimento di Fisica Sperimentale, Università di Torino^b, I-10125 Torino, Italy
- ⁷⁴INFN Sezione di Trieste^a; Dipartimento di Fisica, Università di Trieste^b, I-34127 Trieste, Italy
- ⁷⁵IFIC, Universitat de Valencia-CSIC, E-46071 Valencia, Spain
- ⁷⁶University of Victoria, Victoria, British Columbia, Canada V8W 3P6
- ⁷⁷Department of Physics, University of Warwick, Coventry CV4 7AL, United Kingdom
- ⁷⁸University of Wisconsin, Madison, Wisconsin 53706, USA

We search for the neutrinoless, lepton-flavor-violating tau decays $\tau^- \rightarrow \ell^- V^0$, where ℓ is an electron or muon and V^0 is a vector meson reconstructed as $\phi \rightarrow K^+ K^-$, $\rho \rightarrow \pi^+ \pi^-$, $K^* \rightarrow K^+ \pi^-$, $\bar{K}^* \rightarrow K^- \pi^+$. The analysis has been performed using 451 fb^{-1} of data collected at an e^+e^- center-of-mass energy near 10.58 GeV with the BABAR detector at the PEP-II storage rings. The number of events found in the data is compatible with the background expectation, and upper limits on the branching fractions are set in the range $(2.6 - 19) \times 10^{-8}$ at the 90% confidence level.

PACS numbers: 13.35.Dx, 14.60.Fg, 11.30.Hv

Lepton-flavor violation (LFV) involving tau leptons has never been observed, and recent experimental results have placed stringent limits on the branching frac-

tions for 2- and 3-body, neutrinoless tau decays [1, 2, 3]. Many descriptions of physics beyond the Standard Model (SM) predict such decays [4, 5]; and certain models [6, 7]

specifically predict semileptonic tau decays such as $\tau \rightarrow \ell \phi/\rho/K^*/\bar{K}^*$ ($\tau^- \rightarrow \ell^- V^0$), with rates as high as the current experimental limits [3]. An observation of these decays would be a clear signature of physics beyond the SM, while improved limits will further constraint models of new physics.

This paper presents a search for LFV in a set of eight neutrinoless decay modes $\tau^- \rightarrow \ell^- V^0$ [8], where ℓ is an electron or muon and V^0 is a neutral vector meson decaying to two charged hadrons ($V^0 \rightarrow h^+ h^-$) via one of the following four decay modes: $\phi \rightarrow K^+ K^-$, $\rho \rightarrow \pi^+ \pi^-$, $K^* \rightarrow K^+ \pi^-$, $\bar{K}^* \rightarrow \pi^+ K^-$. A similar search for the non-resonant decays is found in Ref. [2]. This analysis is based on data recorded by the *BABAR* detector at the PEP-II asymmetric-energy e^+e^- storage rings operated at the SLAC National Accelerator Laboratory. The data sample consists of 410 fb^{-1} recorded at e^+e^- center-of-mass (c.m.) energy $\sqrt{s} = 10.58 \text{ GeV}$, and 40.8 fb^{-1} recorded at $\sqrt{s} = 10.54 \text{ GeV}$. With a calculated cross section for tau pairs of $\sigma_{\tau\tau} = 0.919 \pm 0.003 \text{ nb}$ [9, 10] at the stated luminosity-weighted \sqrt{s} , this data set corresponds to the production of about 830 million tau decays.

The *BABAR* detector is described in detail in Ref. [11]. Charged-particle (track) momenta are measured with a 5-layer double-sided silicon vertex tracker and a 40-layer helium-isobutane gas drift chamber inside a 1.5-T superconducting solenoidal magnet. An electromagnetic calorimeter consisting of 6580 CsI(Tl) crystals is used to identify electrons and photons, and a ring-imaging Cherenkov detector (DIRC) is used to identify charged hadrons. The instrumented magnetic flux return (IFR) is embedded with limited streamer tubes and resistive plate chambers, and is used to identify muons.

We use a Monte Carlo (MC) simulation of lepton-flavor-violating tau decays to optimize the search. Tau-pair events including higher-order radiative corrections are generated using *KK2f* [10]. One tau decays to a lepton and a vector meson, with the meson decaying according to the measured branching fractions [12], while the other tau decays via SM processes simulated with *Tauola* [13]. Final state radiative effects are simulated for all decays using *Photos* [14]. The detector response is modeled with *GEANT4* [15], and the simulated events are then reconstructed in the same manner as data. SM background processes are modeled with a similar software framework.

We search for the signal decay $\tau^- \rightarrow \ell^- V^0 \rightarrow \ell^- h^+ h^-$ by reconstructing $e^+e^- \rightarrow \tau^+\tau^-$ candidates in which three charged particles, each identified as the appropriate lepton or hadron, have an invariant mass and energy close to that of the parent tau lepton. Candidate signal events are first required to have a “3-1 topology,” where one tau decay yields three charged particles, while the second tau decay yields one charged particle. This requirement on the second tau decay greatly reduces the background from continuum multi-hadron events. Events with four well-reconstructed tracks and zero net charge

are selected, and the tracks are required to point toward a common region consistent with $\tau^+\tau^-$ production and decay. The polar angle of all four tracks in the laboratory frame is required to be within the calorimeter acceptance. Pairs of oppositely-charged tracks are ignored if their invariant mass, assuming electron mass hypotheses, is less than $30 \text{ MeV}/c^2$. Such tracks are likely to be from photon conversions in the traversed material. The event is divided into hemispheres in the e^+e^- c.m. frame using the plane perpendicular to the thrust axis, as calculated from the observed tracks and neutral energy deposits. The signal (3-prong) hemisphere must contain exactly three tracks while the other (1-prong) hemisphere must contain exactly one.

Each of the charged particles found in the 3-prong hemisphere must be identified as a lepton or hadron candidate appropriate to the LFV decay for each search channel. Electrons are identified using the ratio of calorimeter energy to track momentum (E/p), the ionization loss in the tracking system (dE/dx), and the shape of the shower in the calorimeter. Muon identification makes use of a neural network, inputs to which include the number of signals in the IFR, the number of interaction lengths traversed, and the energy deposition in the calorimeter. Pions and kaons are identified by their energy loss in the tracking system, and by the Cherenkov angle and the number of photons observed in the DIRC.

To further suppress backgrounds from quark pair production, Bhabha scattering events, and SM tau pair production, we apply additional selection criteria separately in the eight different search channels. Resonant decays are selected with cuts on the invariant mass of the two hadrons in the 3-prong hemisphere. The invariant mass of the 1-prong hemisphere is calculated from the charged and neutral particles in that hemisphere and the total missing momentum in the event. As the missing momentum in signal events results from one or more neutrinos in the 1-prong hemisphere, this mass is constrained to be near the tau mass. Background events from quark pair production are suppressed with cuts on the total transverse momentum in the event, the scalar sum of all transverse momenta in the c.m. frame, and the number of photons in the 1-prong and 3-prong hemispheres. To reduce the background contribution from radiative Bhabha and di-muon events, cuts are made on the cosine of the acolinearity angle between the 1-prong and 3-prong momentum vectors in the c.m. frame. Furthermore, the 1-prong track must not be identified as an electron for the $\tau^- \rightarrow e^- \rho$ search. All selection criteria are optimized in each search channel to provide the smallest expected upper limit on the branching fraction in the background-only hypothesis.

As a final discriminant, we require candidate signal events to have an invariant mass and total energy in the 3-prong hemisphere consistent with a parent tau lepton. These quantities are calculated from the measured

track momenta, assuming lepton and hadron masses that correspond to the neutrinoless tau decay in each search channel. The energy difference is defined as $\Delta E \equiv E_{\text{rec}}^* - E_{\text{beam}}^*$, where E_{rec}^* is the total energy of the tracks observed in the 3-prong hemisphere and E_{beam}^* is the beam energy, with both quantities calculated in the c.m. frame. The mass difference is defined as $\Delta M \equiv M_{\text{EC}} - m_\tau$ where M_{EC} is calculated from a kinematic fit to the 3-prong track momenta with the energy constrained to be $\sqrt{s}/2$ in the c.m. frame, and $m_\tau = 1.777 \text{ GeV}/c^2$ is the tau mass [12]. While the energy constraint significantly reduces the spread of ΔM values, it also introduces a correlation between ΔM and ΔE , which must be taken into account when fitting distributions in this 2-dimensional space.

Detector resolution and radiative effects broaden the signal distributions in the $(\Delta M, \Delta E)$ plane. Because of the correlation between ΔM and ΔE , the radiation of photons from the incoming e^+e^- particles produces a tail at positive values of ΔM and negative values of ΔE . Radiation from the final-state leptons, which is more likely for electrons than muons, leads to a tail at low values of ΔE . Rectangular signal boxes (SB) in the $(\Delta M, \Delta E)$ plane are defined separately for each search channel. As with previous selection criteria, the SB boundaries are chosen to provide the smallest expected upper limit on the branching fraction. The expected upper limit is estimated using only MC simulations and data events in the sideband region, as described below. Fig. 1 shows the observed data in the Large Box (LB) of the $(\Delta M, \Delta E)$ plane, along with the SB boundaries and the expected signal distributions. While a small fraction of the signal events lie outside the SB, the effect on the final result is negligible. To avoid bias, we use a blinded analysis procedure with the number of data events in the SB remaining unknown until the selection criteria are finalized and all crosschecks are performed.

There are three main classes of background remaining after the selection criteria are applied: charm quark production ($c\bar{c}$), low-multiplicity continuum $e^+e^- \rightarrow u\bar{u}/d\bar{d}/s\bar{s}$ events (uds), and SM $\tau^+\tau^-$ pair events. These three background classes have distinctive distributions in the $(\Delta M, \Delta E)$ plane. The uds events tend to populate the plane evenly, with a fall-off at positive values of ΔE . Events in the $c\bar{c}$ sample exhibit peaks at positive values of ΔM due to D and D_s mesons, and are generally restricted to negative values of ΔE . The $\tau^+\tau^-$ background events are restricted to negative values of both ΔE and ΔM .

The expected background rates in the SB are determined by fitting a set of 2-dimensional probability density functions (PDFs) to the observed data in the grand sideband (GS) region of the $(\Delta M, \Delta E)$ plane. The GS region is defined as the LB minus the SB. The shapes of the PDFs are determined by fits to the $(\Delta M, \Delta E)$ distributions of background MC samples in the LB, as

described in Ref. [1]. The present analysis makes use of the same parameterization as Ref. [1] for the ΔE spectra, except for the case of the $c\bar{c}$ spectrum in some search channels. In these cases, combinations of polynomial and Gaussian functions are used. The choice of PDF for the ΔM spectrum of the uds samples is the same as used in Ref. [1], while the $\tau^+\tau^-$ and $c\bar{c}$ ΔM spectra are modeled with Gaussian and polynomial functions, or the Crystal Ball function [16]. All shape parameters, including a rotation angle accounting for the correlation between ΔE and ΔM , are determined from the fits to MC samples.

Once the shapes of the three background PDFs are determined, an unbinned extended maximum likelihood fit to the data in the GS region is used to find the expected background count in the SB. The fits to the background MC samples and to data are performed separately for each of the eight search channels.

We estimate the signal event selection efficiency with a MC simulation of lepton-flavor violating tau decays. Between 20% and 40% of the MC signal events pass the 3-1 topology requirement. The efficiency for identification of the three final-state particles ranges from 42% for $\tau^- \rightarrow \mu^- K^*$ to 82% for $\tau^- \rightarrow e^- \rho$. The total efficiency for signal events to be found in the SB is shown in Table I, and ranges from 4.1% to 8.0%. This efficiency includes the branching fraction for the vector meson decay to charged daughters, as well as the branching fraction for 1-prong tau decays.

The particle identification efficiencies and misidentification probabilities have been measured with control samples both for data and MC events, as a function of particle momentum, polar angle, and azimuthal angle in the laboratory frame. The systematic uncertainties related to the particle identification have been estimated from the statistical uncertainty of the efficiency measurements and from the difference between data and MC efficiencies. These uncertainties range from 1.7% for $\tau^- \rightarrow e^- \rho$ to 9.0% for $\tau^- \rightarrow \mu^- \rho$ [17]. The modeling of the tracking efficiency and the uncertainty from the 1-prong tau branching fraction each contribute an additional 1% uncertainty. Furthermore, the uncertainty on the intermediate branching fractions $\mathcal{B}(\phi/K^*/\bar{K}^* \rightarrow h^+h^-)$ contributes a 1% uncertainty. All other sources of uncertainty in the signal efficiency are found to be negligible, including the statistical limitations of the MC signal samples, modeling of radiative effects by the generator, track momentum resolution, trigger performance, and the choice of observables used in the selection criteria.

Since the background levels are extracted directly from the data, systematic uncertainties on the background estimation are directly related to the background parameterization and the fit technique used. Uncertainties related to the fits to the background samples are estimated by varying the background shape parameters according to the covariance matrix and repeating the fits, and range

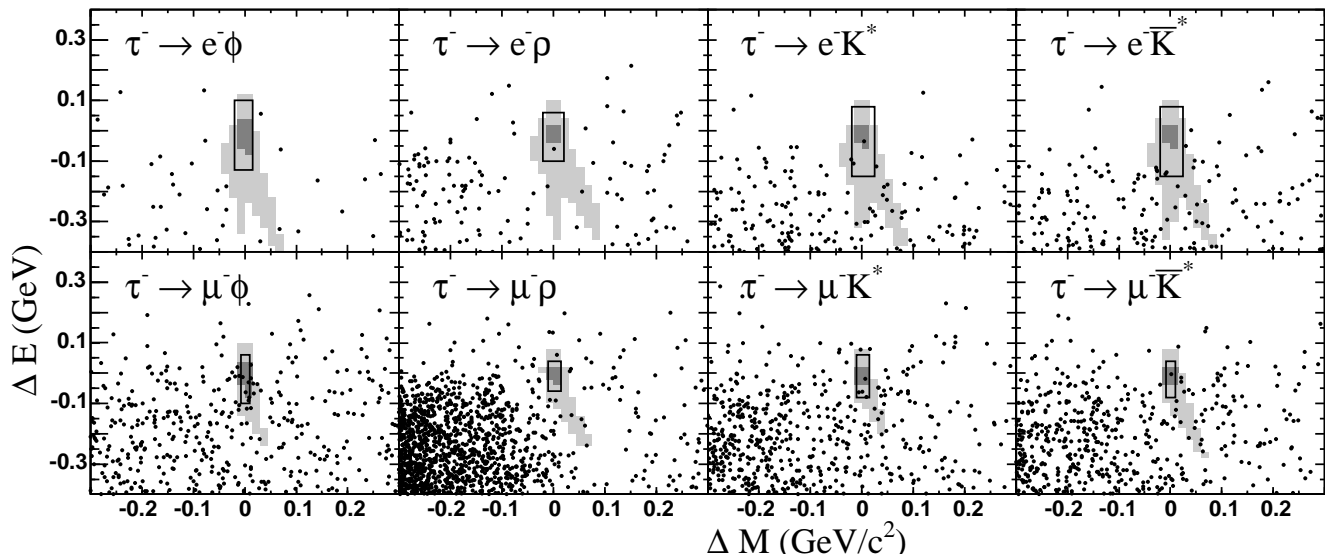


FIG. 1: Observed data shown as dots in the Large Box of the $(\Delta M, \Delta E)$ plane and the boundaries of the Signal Box. The dark and light shading indicates contours containing 50% and 90% of the selected MC signal events, respectively.

TABLE I: Efficiency estimate, number of expected background events (N_{bgd}), number of observed events (N_{obs}), observed upper limit at 90% CL on the number of signal events (N_{UL}^{90}), expected branching fraction upper limit at 90% CL ($\mathcal{B}_{\text{exp}}^{90}$), and observed branching fraction upper limit at 90% CL ($\mathcal{B}_{\text{UL}}^{90}$). $\mathcal{B}_{\text{exp}}^{90}$ and $\mathcal{B}_{\text{UL}}^{90}$ are in units of 10^{-8} .

Mode	ε [%]	N_{bgd}	N_{obs}	N_{UL}^{90}	$\mathcal{B}_{\text{exp}}^{90}$	$\mathcal{B}_{\text{UL}}^{90}$
$e\phi$	6.43 ± 0.16	0.68 ± 0.12	0	1.8	5.0	3.1
$\mu\phi$	5.18 ± 0.27	2.76 ± 0.16	6	8.7	8.2	19
$e\rho$	7.31 ± 0.18	1.32 ± 0.17	1	3.1	4.9	4.6
$\mu\rho$	4.52 ± 0.41	2.04 ± 0.19	0	1.1	8.9	2.6
eK^*	8.00 ± 0.19	1.65 ± 0.23	2	4.3	4.8	5.9
μK^*	4.57 ± 0.36	1.79 ± 0.21	4	7.1	8.5	17
$e\bar{K}^*$	7.76 ± 0.18	2.76 ± 0.28	2	3.2	5.4	4.6
$\mu\bar{K}^*$	4.11 ± 0.32	1.72 ± 0.17	1	2.7	9.3	7.3

from 3.8% to 10%. Uncertainties related to the fits for the background yields in the GS are estimated by varying the yields within their errors, and range from 4.1% to 16%. The total uncertainty on the background estimates is shown in Table I. Crosschecks of the background estimation are performed by comparing the number of events expected and observed in sideband regions immediately neighboring the SB for each search channel. No major discrepancies are observed.

The number of events observed (N_{obs}) and the number of background events expected (N_{bgd}) are shown in Table I. The POLE calculator [18], based on the method of Feldman and Cousins [19], is used to place 90% CL upper limits on the number of signal events (N_{UL}^{90}), which include uncertainties on N_{bgd} and on the selection efficiency (ε). For the $\tau^- \rightarrow \mu^- \phi$ search, the POLE cal-

culcation results in a two-sided interval at 90% CL for the number of signal events: $[0.39 - 8.65]$. Upper limits on the branching fractions are calculated according to $\mathcal{B}_{\text{UL}}^{90} = N_{\text{UL}}^{90} / (2\varepsilon L \sigma_{\tau\tau})$, where the values L and $\sigma_{\tau\tau}$ are the integrated luminosity and $\tau^+\tau^-$ cross section, respectively. The uncertainty on the product $L\sigma_{\tau\tau}$ is 1.0%. Table I lists the upper limits on the branching fractions, as well as the expected upper limit $\mathcal{B}_{\text{exp}}^{90}$, defined as the mean upper limit expected in the background-only hypothesis. The 90% CL upper limits on the $\tau \rightarrow \ell \phi/\rho/K^*/\bar{K}^*$ branching fractions are in the range $(2.6 - 19) \times 10^{-8}$, and these limits represent improvements over the previous experimental bounds [3] in almost all search channels.

We are grateful for the excellent luminosity and machine conditions provided by our PEP-II colleagues, and for the substantial dedicated effort from the computing organizations that support BABAR. The collaborating institutions wish to thank SLAC for its support and kind hospitality. This work is supported by DOE and NSF (USA), NSERC (Canada), CEA and CNRS-IN2P3 (France), BMBF and DFG (Germany), INFN (Italy), FOM (The Netherlands), NFR (Norway), MES (Russia), MEC (Spain), and STFC (United Kingdom). Individuals have received support from the Marie Curie EIF (European Union) and the A. P. Sloan Foundation.

* Deceased

† Now at Temple University, Philadelphia, Pennsylvania 19122, USA

‡ Now at Tel Aviv University, Tel Aviv, 69978, Israel

§ Also with Università di Perugia, Dipartimento di Fisica,

Perugia, Italy

- ¶ Also with Università di Roma La Sapienza, I-00185 Roma, Italy
 - ** Now at University of South Alabama, Mobile, Alabama 36688, USA
 - †† Also with Laboratoire de Physique Nucléaire et de Hautes Energies, IN2P3/CNRS, Université Pierre et Marie Curie-Paris6, Université Denis Diderot-Paris7, F-75252 Paris, France
 - ‡‡ Also with Università di Sassari, Sassari, Italy
- [1] BABAR Collaboration, B. Aubert *et al.*, Phys. Rev. Lett. **99**, 251803 (2007).
- [2] BABAR Collaboration, B. Aubert *et al.*, Phys. Rev. Lett. **95**, 191801 (2005).
- [3] Belle Collaboration, Y. Nishio *et al.*, Phys. Lett. B **664**, 35 (2008).
- [4] P. Paradisi, JHEP **0510**, 006 (2005).
- [5] A. Brignole and A. Rossi, Phys. Lett. B **566**, 217 (2003).
- [6] A. Brignole and A. Rossi, Nucl. Phys. B **701**, 4 (2004).
- [7] E. Arganda, J.M. Herrero, J. Portoles, JHEP **0806**, 079 (2008).
- [8] Throughout this paper, charge conjugate decay modes are implied.
- [9] S. Banerjee *et al.*, Phys. Rev. D **77**, 054021 (2008).
- [10] S. Jadach, B. F. L. Ward, and Z. Wąs, Comput. Phys. Commun. **130**, 260 (2000).
- [11] BABAR Collaboration, B. Aubert *et al.*, Nucl. Instrum. Methods Phys. Res., Sect. A **479**, 1 (2002).
- [12] Particle Data Group, Y.-M. Yao *et al.*, J. Phys. **G33**, 1 (2006).
- [13] S. Jadach *et al.*, Comput. Phys. Commun. **76**, 361 (1993).
- [14] E. Barberio and Z. Wąs, Comput. Phys. Commun. **79**, 291 (1994).
- [15] GEANT4 Collaboration, S. Agostinelli *et al.*, Nucl. Instrum. Methods Phys. Res., Sect. A **506**, 250 (2003).
- [16] M.J. Oreglia, Ph.D Thesis, SLAC-236(1980), Appendix D; J.E. Gaiser, Ph.D Thesis, SLAC-255(1982), Appendix F; T. Skwarnicki, Ph.D Thesis, DESY F31-86-02(1986), Appendix E.
- [17] All uncertainties quoted in the text are relative.
- [18] J. Conrad *et al.*, Phys. Rev. D **67**, 012002 (2003).
- [19] G. J. Feldman and R. D. Cousins, Phys. Rev. D **57**, 3873 (1998).